

Contrasting Freezeouts in Large Versus Small Systems

Sandeep Chatterjee, Ajay Kumar Dash and Bedangadas Mohanty

School of Physical Sciences,
National Institute of Science Education and Research, Jatni-752050, India

E-mail: sandeepc@niser.ac.in, ajayd@niser.ac.in and bedanga@niser.ac.in

Abstract. We study the data on mean hadron yields and contrast the chemical freezeout conditions in p+p, p+Pb and Pb+Pb at the Large Hadron Collider (LHC) energies. We study several schemes for freezeout that mainly differ in the way strangeness is treated: i. strangeness freezes out along with the non-strange hadrons in complete equilibrium (1CFO), ii. strangeness freezes out along with non-strange hadrons with an additional parameter γ_S accounting for non-equilibrium production of strangeness (1CFO+ γ_S), and iii. strangeness freezes out earlier than non-strange hadrons and in thermal equilibrium (2CFO). A comparison of the chisquares of the fits indicate a dependence of the freezeout scheme on the system size. The minimum bias p+p and different centralities of p+Pb and peripheral Pb+Pb data prefer 1CFO+ γ_S with γ_S approaching unity as we go from p+p to central p+Pb and peripheral Pb+Pb. On the other hand, the mid-central to central Pb+Pb data prefer 2CFO over 1CFO+ γ_S . Such system size dependence of freezeout scheme could be an indication of the additional interaction in Pb+Pb over p+Pb and p+p.

1. Introduction

A hot and dense strongly interacting medium, the fireball, is produced in ultra-relativistic heavy ion collisions (HICs). Assuming rapid thermalization, the ensuing expansion phase has been modelled by relativistic hydrodynamics with considerable success [1]. The expansion of the fireball causes dilution of the energy density of the system. The medium mean free path elongates and finally drives the fireball out of equilibrium. The analysis of the hadron yields allows an access to the properties of the chemical freezeout (CFO) surface where the hadronic inelastic collisions ceased [2, 3, 4, 5]. There are on going efforts to extract the CFO surface not only from the measured mean hadron yields but also from their higher order moments through the measurement of event by event (e-by-e) fluctuations of the QCD conserved charges [6, 7, 8, 9, 10, 11].

A unified CFO scheme where all the hadrons freezeout together, parametrised by a single temperature, baryon chemical potential and volume of the freezeout surface (1CFO) have been widely used to describe the hadron yields across a wide range of $\sqrt{s_{\text{NN}}}$ [2, 3, 4, 5]. The extracted CFO surface from these analyses was found in close proximity to the hadronization surface as indicated by lattice QCD studies at zero net-baryon densities [12]. This led to several suggestions like the hadrons are born directly into equilibrium at the time of hadronization [13] or the multi-particle interactions that maintain equilibrium are relevant only close to the hadronization surface [14]. However, the absence of an unambiguous microscopic description of the freeze-out dynamics and that the interaction cross-sections among various hadrons in the system not playing a manifestly important role left a sense of incompleteness in the 1CFO approach. In addition, it was observed that this approach is reasonably well applicable to $e^+ + e^-$, p+p and A+A collisions [15], raising questions as to the sensitivity of the 1CFO scheme to the differences in the underlying interactions as expected for such a variety of systems.

It is now well known that the standard 1CFO scheme fails to describe satisfactorily the hadron yields for Pb+Pb collisions at $\sqrt{s_{\text{NN}}} = 2.76$ TeV [16] which was termed as ‘proton anomaly’ [17] and also interpreted as tension in the non-strange vs strange sectors [18, 19, 20, 21, 22]. It is to be noted that similar tensions between 1CFO and data exist even at lower $\sqrt{s_{\text{NN}}}$ [23, 20, 22, 24]. There have been suggestions to describe the hadron yields at the LHC- incorporating effects of non-equilibrium evolution either through a microscopic hadronic afterburner [25, 26] or through additional flavor dependent fugacity factors [27, 28, 29] within the 1CFO scheme. It has been further suggested that the current discrepancy between models and data could be due to missing resonances in the models that have not been observed yet but are expected from QCD models and LQCD computations [30, 31]. A flavor dependent sequential freezeout scheme with different freezeout surfaces for hadrons with zero and non-zero strangeness content (2CFO) was also suggested based on flavor dependence in several thermodynamic quantities in LQCD computations [19] and known systematics of hadron cross-sections [20]. The 2CFO scheme was analysed and was found to provide a much

improved description of the hadron yields [20, 32, 22, 33]. An alternate approach that has successfully described the LHC yields is to consider the Van der Waals excluded volumes for the hadrons with the hadron mass-eigenvolume relationship being flavor dependent [34] (2EV). The χ^2/NDF (NDF=Number of data points - Number of free parameters) for the data-model comparison to the LHC hadron yields, for both the schemes, 2CFO and 2EV are less than unity. Thus, it is not possible to discriminate between these two very different approaches to introduce flavor dependence with yield data alone. Hence, it will be interesting to check how 2EV fares with the data on hadron spectra at the LHC energies as well as at the lower energies. For both these cases, it has been already demonstrated that 2CFO fares better than the conventional 1CFO scheme [20, 33].

Recently it was reported that for p+p collisions at the LHC at $\sqrt{s_{\text{NN}}} = 900$ GeV and 7 TeV, 1CFO+ γ_S performs better than 2CFO [35]. In 1CFO+ γ_S , we still have a unified freezeout for all hadrons, however strangeness is relaxed to go out of equilibrium compared to the rest. γ_S is the additional parameter that accounts for non-equilibrium production of strangeness. This probably hints at a system size dependence in the freezeout scheme where HICs prefer 2CFO while small systems like p+p and p+Pb prefer 1CFO+ γ_S scheme. In this paper we aim to investigate this possible system size dependence in the freezeout scheme in more details. We have analysed the mid-rapidity data for hadron yields in p+p [36, 37, 38], p+Pb [39, 40, 41] and Pb+Pb [42, 43, 44, 45] collisions at $\sqrt{s_{\text{NN}}} = 7, 5.02$ and 2.76 TeV respectively across all the available centralities. In doing so we cover over three orders of magnitudes in terms of the mid-rapidity charged multiplicity as well as the extracted fireball volume at the time of freezeout. This allows us to systematically study the system size dependence of the freezeout conditions. The p+p data at different LHC energies have been previously studied [35]. The thermal freezeout parameters are almost constant across these beam energies. Hence the difference in $\sqrt{s_{\text{NN}}}$ for p+p, p+Pb and Pb+Pb in our study is not expected to affect the conclusions on the role of system size. There have been recent studies on system size dependence of hadron yields at SPS energies [24] and the fate of the maxima in several particle ratios like K^+/π^+ and Λ/π [46].

2. Freezeout Schemes

The primordial yields in the hadron resonance gas model (HRGM) which is used to extract the freezeout conditions in the 1CFO scheme in the Grand Canonical ensemble (GCE) is given by

$$N_i = \frac{g_i V}{2\pi^2} \sum_{k=1}^{\infty} (\pm 1)^{k+1} \frac{m_i^2 T}{k} K_2 \left(\frac{km_i}{T} \right) e^{k\mu_i/T}. \quad (1)$$

Here, V and T are the volume and temperature of the fireball. K_2 is the modified Bessel function of the second kind. g_i , m_i and μ_i refer to the degeneracy factor, mass and hadron chemical potential of the i^{th} hadron species respectively. The total yield

N_i^{tot} is obtained by including the resonance decay contribution to the above primordial yield

$$N_i^{tot} = N_i + \sum_j B.R._{ij} \times N_j \quad (2)$$

where $B.R._{ij}$ is the branching ratio for the j^{th} hadron species to i^{th} hadron species. As of yet, this model has no predictive power since in principle, all the μ_i s are independent of each other. At this stage, a crucial assumption is made of complete chemical equilibrium which allows to parametrise all the μ_i s in terms of only μ_B , μ_Q and μ_S - three chemical potentials corresponding to the three conserved charges of QCD, namely baryon number B , electric charge Q and strangeness S

$$\mu_i = B_i\mu_B + Q_i\mu_Q + S_i\mu_S \quad (3)$$

Now this is a phenomenologically viable model with only T , μ_B and V to fit from data while μ_S and μ_Q are extracted from the conditions of strangeness neutrality and net baryon to net charge ratio of the colliding systems. Thus, 1CFO is expected to work well if all the inelastic hadronic interactions freezeout together, in particular, if all the strangeness changing transmutations cease at the same instant as those that do not involve changing of strangeness.

In 2CFO, we use different freezeout parameters for hadrons with zero and non-zero strangeness content in Eq. 1. We also employ a variant of 2CFO where we reduce one free parameter by imposing entropy conservation between the strange and non-strange freezeout surfaces [32]. The non-strange volume V_{NS} is computed from the entropy conservation constraint in the following way

$$V_{NS}s(T_{NS}, \{\mu\}_{NS}) = V_Ss(T_S, \{\mu\}_S) \quad (4)$$

where s refers to the entropy density and $\{\mu\}$ just refers to the three chemical potentials together: μ_B , μ_S and μ_Q . We label this scheme as 2CFO+FS. The strange hadrons freezeout at the strange freezeout surface. After this, we have only the non-strange hadrons following the $(T, \{\mu\})$ trajectory of the fireball. For entropy conservation between the two freezeouts, the entropy content of the non-strange hadrons post strange freezeout must be equal to the entropy content of the non-strange hadrons prior to the non-strange freezeout. Thus, only the non-strange hadrons contribute to both LHS and RHS of Eq. 4. It is to be noted that the strange resonances decay to strange as well as non-strange hadrons. Thus the non-strange fitted parameters are affected by the strange hadron yields as well.

We have performed our analysis for four different freezeout schemes- 1CFO, 1CFO+ γ_S , 2CFO and 2CFO+FS. The hadrons whose mid-rapidity yields have been fitted to extract the CFO conditions are $\pi^+ + \pi^-$, $K^+ + K^-$, $p + \bar{p}$, ϕ , $\Xi + \bar{\Xi}$ and $\Omega + \bar{\Omega}$ in all the systems. Additionally, we have also used $\Lambda + \bar{\Lambda}$ in p+Pb and only Λ in Pb+Pb. At these energies, the data reveals good particle-antiparticle symmetry allowing us to take the hadron chemical potentials to be zero throughout this work. Thus the parameters to be extracted from the thermal fits in 1CFO are only the fireball

volume V and temperature T at the time of freezeout. In the 1CFO+ γ_S scheme, we treat γ_S also as an additional fitting parameter. In the 2CFO scheme we stay within complete equilibrium setup. However, since we allow for different freezeout thermal parameters for the non-strange and strange hadrons we have four (V_S , T_S , V_{NS} and T_{NS}) parameters. Finally, in 2CFO+FS, we manage to do away with V_{NS} as a fitting parameter using Eq. 4 and thus have only three parameters (V_S , T_S and T_{NS}). Hence, both 1CFO+ γ_S and 2CFO+FS have three free parameters to be fitted from data. Thus, their goodness of fit can be compared unambiguously using the chisquares of the fits.

It has been a standard practice to treat the QCD conserved charges in HICs in the GCE while those of p+p in either canonical ensembles for all the conserved charges (CE) [47] or strangeness alone (SCE) [48]. In QCD, particle production has to obey local charge conservation rules for B , Q and S . Thus, an independent particle production scenario as envisaged within a GCE should receive corrections due to multi-particle correlations introduced through such conservation rules. These corrections are particularly significant in small systems where the total multiplicity itself is small. This calls for different ensembles like CE or SCE in small systems. However, in a QGP state the flavor carrying degrees of freedom are almost massless, allowing for a profuse productions of all the flavors. In such cases, the corrections due to the conservation laws will be small and GCE can provide a good description of particle production even in small systems. Also, at high energies when we only treat the mid-rapidity data, it might be possible to treat the data from small systems like p+p and p+Pb as well in the GCE as we are always observing an open system irrespective of the system size. In a recent work it was pointed out that at the top RHIC and LHC energies, the mid-rapidity p+p data can be better described in the GCE than in CE or SCE [35]. We have checked that the $\chi^2/\text{NDF} \sim 20$ in the CE and SCE while in GCE we find $\chi^2/\text{NDF} \sim 3$. In this paper, we always work in the GCE across all the system sizes in p+p, p+Pb and Pb+Pb.

3. Freezeout in p+p, p+Pb and Pb+Pb

We first compare the quality of fit in different schemes and systems. The goodness of fit in terms of χ^2/NDF (NDF = Number of data points - Number of free parameters) for the different freezeout schemes across different centralities for Pb+Pb, p+Pb and p+p collisions are tabulated in Table 1 and plotted in Fig. 1. In all the schemes the fit quality deteriorates as we go from Pb+Pb to p+Pb and p+p collisions. This is most dramatic for the 2CFO and 2CFO+FS schemes where the χ^2/NDF rises from $\sim 0 - 2$ in Pb+Pb to $\sim 6 - 9$ in p+Pb and p+p. In 1CFO, χ^2/NDF ranges between $2 - 5$ in Pb+Pb while in p+Pb and p+p it varies between $4 - 8$. 1CFO+ γ_S scheme gives largely a constant χ^2/NDF with a very mild rise from Pb+Pb ($\chi^2/\text{NDF} \sim 2 - 3$) to p+Pb and p+p ($\chi^2/\text{NDF} \sim 3 - 4$).

The most important lesson that we learn from Fig. 1 is that the 2CFO freezeout scheme works only for large system size. In large systems, the fireball lifetime is expected

Table 1. The goodness of fits of different models compared. The number of free parameters are 2, 3, 4 and 3 for 1CFO, 1CFO+ γ_S , 2CFO and 2CFO+FS respectively. The number of yield data available for p+p, p+Pb and Pb+Pb are 6, 7 and 7 respectively. Since 1CFO+ γ_S and 2CFO+FS have same number of free parameters, their goodness of fit can be compared unambiguously by simply comparing the chisquares of their fits to data. These columns have been shaded in grey. We observe that 1CFO+ γ_S has smaller chisquare for p+p and p+Pb collisions while 2CFO+FS perform better in Pb+Pb collisions. This points to a plausible system size dependence of freezeout scheme.

System	Centrality %	χ^2				χ^2/NDF			
		1CFO	1CFO+ γ_S	2CFO	2CFO+FS	1CFO	1CFO+ γ_S	2CFO	2CFO+FS
p-p	min-bias	62.6	14.2	24.2	27	15.7	4.7	12.1	9
p-Pb	00-05	18.67	16.72	17.56	18.36	3.7	4.2	5.9	4.6
	05-10	20.06	17.08	17.35	19.90	4	4.3	5.8	5
	10-20	21.44	16.42	19.38	21.40	4.3	4.1	6.5	5.4
	20-40	24.69	18.17	22	24.40	5	4.5	7.3	6.1
	40-60	32.43	17.35	26.74	29.27	6.5	4.3	8.9	7.3
	60-80	39.35	14.58	26.91	31.50	7.9	3.6	9	7.9
	80-100	39.07	10.61	21.46	28	7.8	2.7	7.2	7
Pb-Pb	00-10	17.9	10.59	2.39	3.85	3.6	2.6	0.5	1
	10-20	22.38	12.22	1.52	3.27	4.5	3.1	0.5	0.8
	20-40	27.01	12.57	1.03	2.50	5.4	3.1	0.3	0.6
	40-60	14.38	9.35	2.01	3.57	2.9	2.3	0.7	0.9
	60-80	9.95	8.28	7.6	9.90	2	2.1	2.5	2.5

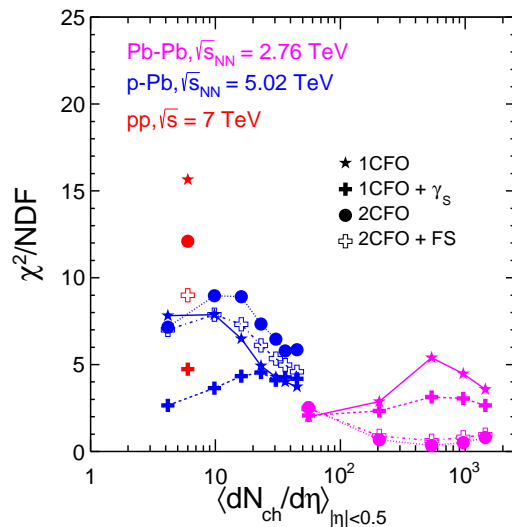


Figure 1. (Color online) The χ^2/NDF for the different freezeout schemes as tabulated in Table 1 have been plotted. It is interesting to note that while 2CFO and its variant 2CFO+FS perform better for $dN_{ch}/d\eta > \sim 10^2$, 1CFO+ γ_S seems to be preferred for lower $dN_{ch}/d\eta$.

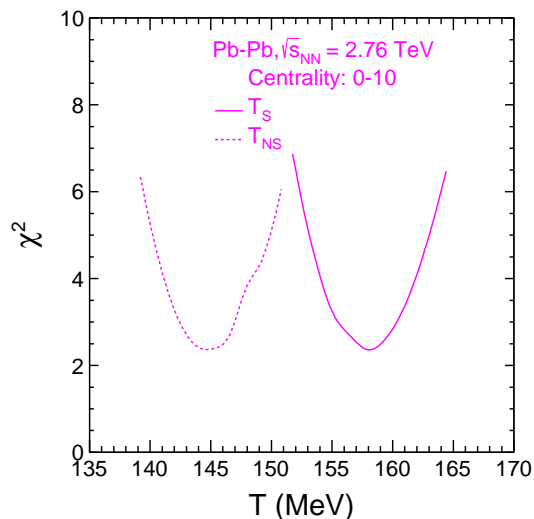


Figure 2. (Color online) The χ^2 vs T for the non-strange and strange freezeout surfaces in 2CFO.

to be long resulting in sufficient interaction amongst constituents and thus the role of hadron-hadron cross sections come into play. The kaons mainly maintain the chemical equilibrium between the non-strange and strange sectors. In a cooling fireball, the kaon to pion ratio rapidly falls resulting in an early freezeout for strangeness [20]. This is the microscopic picture that is the motivation behind the 2CFO scheme. Thus, high rate of hadronic interactions resulting in a hadronic medium formation is essential for 2CFO to work. On the other hand, in small systems the fireball lifetime is much shorter as the expansion dynamics is dominant resulting in little hadronic interactions. Thus the hierarchy in hadron-hadron cross-sections do not enter the freezeout dynamics and we have a sudden freezeout scenario with all the hadrons freezing out together.

In order to understand whether the better performance of 2CFO over 1CFO+ γ_S is merely due to more free parameters, we have also performed the fits in 2CFO+FS which has the same number of free parameters as 1CFO+ γ_S and hence any difference in the chisquares of 2CFO+FS and 1CFO+ γ_S is solely due to the difference in the freezeout scheme of strangeness. As seen in Table 1 and Fig. 1, the performance of 2CFO+FS is better than 1CFO+ γ_S in Pb+Pb while the latter performs better in p+Pb and p+p collisions. This strongly suggests a system size dependence in the freezeout scheme of strangeness. Since 2CFO and 2CFO+FS provide similar results of fits to hadron yield data, henceforth we will only show the results from 2CFO.

We will now investigate the stability of our fits in 2CFO. Pions and protons are the only hadrons with zero strangeness content whose yields are available in the experiments. This might render the extraction of two parameters, T_{NS} and V_{NS} unstable from the fits to data. However, as mentioned earlier, the heavier strange resonances decay to strange as well as non-strange hadrons. This couples the non-strange freezeout parameters to the strange hadron yields as well and allows for a reliable extraction of the freezeout

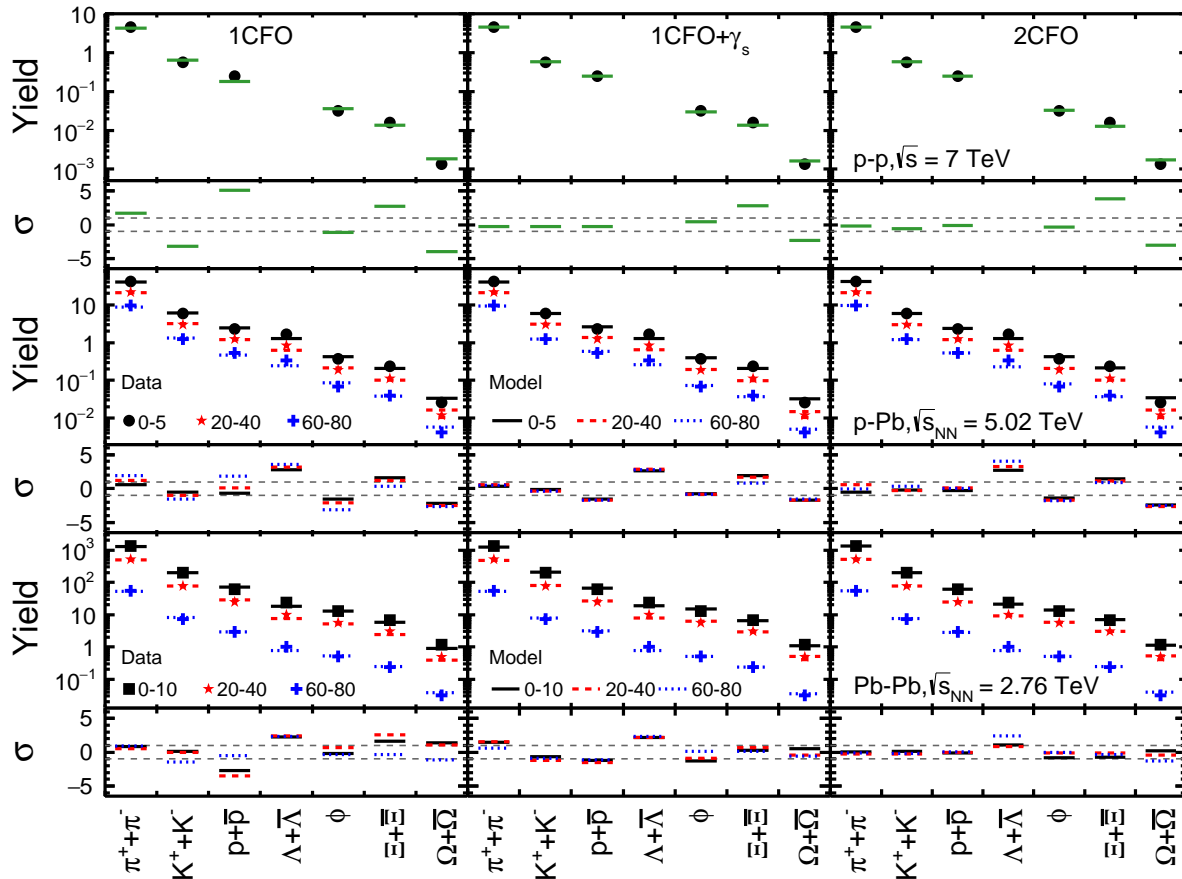


Figure 3. (Color online) The comparison between data [36, 37, 38, 39, 40, 41, 42, 43, 44, 45] and model for p+p (top row) [36, 37, 38], p+Pb (middle row) [39, 40, 41] and Pb+Pb (bottom row) [42, 43, 44, 45] systems in three different freezeout schemes: 1CFO (left column), 1CFO+ γ_s (middle column) and 2CFO (right column). Note that for Pb+Pb the $\Lambda + \bar{\Lambda}$ column refer to only Λ as data for $\bar{\Lambda}$ is not available. Also shown are the deviation of the data from the model (Eq. 5) for each freezeout scheme.

parameters. As seen in Fig. 2, the χ^2 vs T profile for the non-strange and strange freezeout surfaces exhibit a narrow parabola like structure with their minima well separated indicating a clear hint of separate freezeouts of the non-strange and strange hadrons.

We have plotted the measured hadron yields in min-bias p+p [36, 37, 38] and different centralities of p+Pb [39, 40, 41] and Pb+Pb [42, 43, 44, 45] collisions and compared with the thermal model fits for the three freezeout schemes in Fig. 3. For clarity, we show results for only three centralities in p+Pb and Pb+Pb, representing central, mid-central and peripheral collisions. In the lower panel of each figure, we have also shown the deviation σ given by

$$\sigma = \frac{\text{Data} - \text{Model}}{\text{Error of Data}}. \quad (5)$$

In p+p, the 1CFO scheme fares poorly with $\sigma > 5$ for proton. The 1CFO+ γ_s and 2CFO schemes seem to fare equally good, however the multi-strange baryons Ξ and

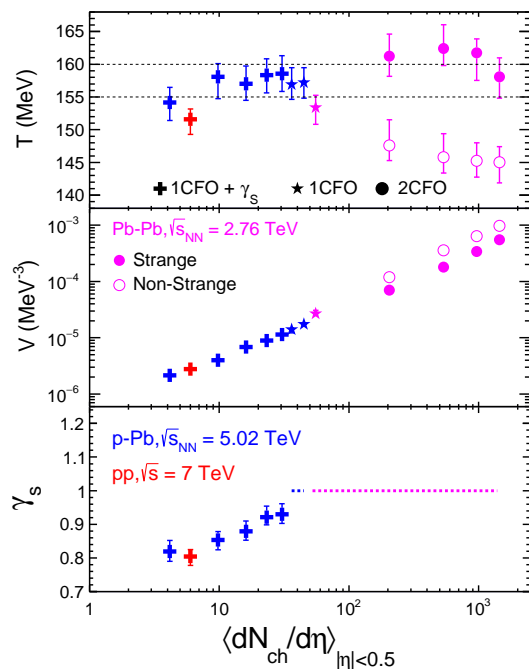


Figure 4. (Color online) The best fitted freezeout parameters (temperature T , volume V and strangeness non-equilibrium factor γ_s) amongst the three different freezeout schemes.

Ω have $\sigma > 2$. Similar situation as in p+p prevails through peripheral to mid-central p+Pb collisions. There is considerable tension both in the mesonic as well as baryonic sectors in the 1CFO scheme which improves as we include γ_s in the 1CFO+ γ_s scheme. The situation changes slightly for the central bins. Here the non-strange sector fares much better in the 1CFO scheme while the $\sigma \sim 2$ in the strange sector do not go away with more free parameters in the 1CFO+ γ_s and 2CFO schemes. In the 2CFO scheme with one more free parameter the agreement for proton betters but at the cost of ϕ mesons. Overall we don't gain by including an extra parameter in 2CFO as compared to 1CFO+ γ_s .

We now turn our attention to the bottom row of Fig. 3 where we have shown results for the Pb+Pb case. The scenario for the most peripheral Pb+Pb bin is similar to the central p+Pb bins. All the schemes exhibit similar goodness of fit and the gain in improving the fit marginally in going from 1CFO to other schemes is compensated by the additional free parameters required. The other centralities exhibit strong tension between the non-strange and strange baryons in 1CFO. In 1CFO+ γ_s , the agreement for the strange baryons improve but the tension between proton and Λ continues while a mild tension between π and kaons develop. Unlike in p+p and p+Pb, we find an appreciable improvement in the fits in 2CFO, only Λ shows a mild deviation of $\sigma \sim 1$.

In Fig. 4 we have plotted the freezeout parameters that provide the best description to the data amongst the three different freezeout schemes that we have studied here. The freezeout temperature stays around 155 – 160 MeV for p+p, p+Pb and also for

the strange hadrons in Pb+Pb collisions. However, the non-strange hadrons in Pb+Pb breakaway from this trend. The higher rate of interaction in the strongly interacting hadronic medium causes a delayed freezeout for them and they finally freezeout at temperatures which are lower by about 10% than those of the strange freezeout surface. All the centralities except the most peripheral bin of (60 – 80)% centrality in Pb+Pb is best described by 2CFO. The non strange freezeout temperature monotonically rises as one goes from central to peripheral bins and merge with its strange companion in the (60 – 80)% centrality bin. The (60 – 80)% centrality bin in Pb+Pb and the two most central bins of (0 – 5)% and (5 – 10)% of p+Pb are best described by the 1CFO scheme. For the rest of the centralities in p+Pb and p+p, it is essential to fit γ_S . Within the 1CFO+ γ_S scheme, the extracted γ_S in p+Pb varies from 0.95 – 0.80 for (10 – 20)% to (80 – 100)% centrality bins. We note here that unlike in the Pb+Pb case, this is more in accordance with expectation from the core-corona picture where the decreasing trend of γ_S can be understood as the decreasing contribution of the core of the colliding Pb ion as one goes from central to peripheral p+Pb bins. The p+p freezeout conditions are in agreement with that of peripheral p+Pb.

The temperatures extracted in HICs can be contrasted to those obtained using the e-by-e fluctuation measures and the hadronisation temperature computed by Lattice QCD. The freeze-out temperature obtained from analysis of fluctuation measure involving dominantly non-strange hadrons for Au+Au collisions at top RHIC energy is $\sim 144 \pm 6$ MeV [8, 9] and is in agreement with the freeze-out temperature from 2CFO for non-strange hadrons in Pb+Pb collisions reported here. The hadronization temperatures reported by LQCD calculations at zero μ_B in Ref. [12] using strange-quark number susceptibilities are found to be closer to the freeze-out temperature reported here for strange hadrons, while hadronization temperature calculated using chiral condensates gives a value which is closer to the freeze-out temperature reported here for non-strange hadrons. However it may be noted that the systematic errors associated with the LQCD results are quite large.

4. Summary and Outlook

We have studied the system size dependence in the CFO conditions in p+p, p+Pb and Pb+Pb collisions at the LHC. Our study confirms that the analysis of the hadron yields within thermal models is sensitive to the physics of the CFO and the χ^2/NDF is a good measure to discriminate between the different CFO scenarios. If the analysis technique was blind to the underlying physics of the different CFO scenarios, one would expect 2CFO to perform the best across all system sizes as it has the highest number of free parameters amongst all the three CFO scenarios studied here. However, we explicitly show that this is not the case. 2CFO performs best only in large system sizes with $dN_{ch}/d\eta > 100$. For smaller systems, 2CFO clearly performs worse than the other scenarios. The varying interplay of expansion and interaction amongst the fireball constituents in Pb+Pb versus p+Pb and p+p could give rise to the above system size

dependence in freezeout.

5. Acknowledgement

SC acknowledges discussions and collaborations on freezeout with Rohini Godbole and Sourendu Gupta. SC and AKD thank XIIth plan project no. 12-R&D-NIS-5.11-0300 of Govt. of India for support. BM acknowledges support from DST SwarnaJayanti and DAE-SRC projects of Govt. of India.

References

- [1] U. W. Heinz and R. Snellings, *Annu. Rev. Nucl. Part. Sci.* **63**, 123-151 (2013).
- [2] P. Braun-Munzinger *et al.*, *Phys. Lett.* **B 365**, 1 (1996).
- [3] G. D. Yen and M. I. Gorenstein, *Phys. Rev.* **C 59**, 2788 (1999).
- [4] F. Becattini *et al.*, *Phys. Rev.* **C 64**, 024901 (2001).
- [5] A. Andronic, P. Braun-Munzinger and J. Stachel, *Nucl. Phys.* **A 772**, 167-199 (2006).
- [6] A. Bazavov *et al.*, *Phys. Rev. Lett.* **109**, 192302 (2012).
- [7] S. Borsanyi *et al.*, *Phys. Rev. Lett.* **111**, 062005 (2013).
- [8] S. Borsanyi *et al.*, *Phys. Rev. Lett.* **113**, 052301 (2014).
- [9] P. Alba, *et al.* *Phys. Lett.* **B 738**, 305-310 (2014).
- [10] A. Bazavov *et al.*, *Phys. Rev.* **D93**, 014512 (2016).
- [11] J. Noronha-Hostler *et al.*, arXiv:1607.02527 [hep-ph].
- [12] G. Endrodi *et al.*, *JHEP* **1104**, 001 (2011).
- [13] R. Stock, *Phys. Lett.* **B456** 277-282 (1999).
- [14] P. Braun-Munzinger, J. Stachel and C. Wetterich, *Phys. Lett.* **B 596**, 61-69 (2004).
- [15] F. Becattini *et al.*, *Eur. Phys. J.* **C66**, 377-386, (2010).
- [16] J. Stachel *et al.*, *J. Phys. Conf. Ser.* **509**, 012019 (2014).
- [17] M. Rybczynski, W. Florkowski and W. Broniowski, *Phys. Rev.* **C85**, 054907 (2012).
- [18] R. Preghenella (ALICE), *Acta Phys. Polon.* **B43**, 555 (2012).
- [19] R. Bellwied *et al.*, *Phys. Rev. Lett.* **111**, 202302 (2013).
- [20] S. Chatterjee, R. Godbole, and S. Gupta, *Phys. Lett.* **B727**, 554 (2013).
- [21] M. Floris, *Nucl. Phys.* **A931**, 103 (2014).
- [22] S. Chatterjee and B. Mohanty, *Phys. Rev.* **C90**, 034908 (2014).
- [23] F. Becattini, J. Manninen and M. Gazdzicki, *Phys. Rev.* **C73**, 044905 (2006).
- [24] V. Vovchenko, V. V. Begun and M. I. Gorenstein, *Phys. Rev.* **C93**, 064906 (2016).
- [25] J. Steinheimer, J. Aichelin, and M. Bleicher, *Phys. Rev. Lett.* **110**, 042501 (2013).
- [26] F. Becattini *et al.*, *Phys. Rev. Lett.* **111**, 082302 (2013).
- [27] M. Petran, J. Letessier, V. Petracek and J. Rafelski, *Phys. Rev.* **C88**, 034907 (2013).
- [28] V. Begun, W. Florkowski and M. Rybczynski, *Phys. Rev.* **C90**, 014906 (2014).
- [29] V. Begun, W. Florkowski, and M. Rybczynski, *Phys. Rev.* **C90**, 054912 (2014).
- [30] A. Bazavov *et al.*, *Phys. Rev. Lett.* **113**, 072001 (2014).
- [31] J. Noronha-Hostler and C. Greiner, arXiv:1405.7298 [nucl-th].
- [32] K. A. Bugaev *et al.*, *Europhys. Lett.* **104** 22002 (2013).
- [33] S. Chatterjee, B. Mohanty and R. Singh, *Phys. Rev.* **C92**, 024917 (2015).
- [34] P. Alba *et al.*, arXiv:1606.06542 [hep-ph].
- [35] S. Das *et al.*, *Phys. Rev.* **C95**, 014912 (2017).
- [36] J. Adam *et al.* (ALICE), *Eur. Phys. J.* **C75** 226 (2015).
- [37] B. Abelev *et al.* (ALICE), *Eur. Phys. J.* **C72** 2183 (2012).
- [38] B. Abelev *et al.* (ALICE), *Phys. Lett.* **B712** 309-318 (2012).

- [39] B. Abelev *et al.* Phys. Lett. **B728** 25-38 (2014).
- [40] J. Adam *et al.* (ALICE), Eur. Phys. J. **C76** 245 (2016).
- [41] J. Adam *et al.* (ALICE), Phys. Lett. **B758** 389-401 (2016).
- [42] B. Abelev *et al.* (ALICE), Phys. Rev. **C88**, 044910 (2013).
- [43] B. Abelev *et al.* Phys. Rev. **C91**, 024609 (2015).
- [44] B. Abelev *et al.* Phys. Rev. Lett. **111**, 222301 (2013).
- [45] B. Abelev *et al.* (ALICE), Phys. Lett. **B728** 216-227 (2014).
- [46] Oeschler *et al.*, arXiv:1603.09553.
- [47] I. Kraus *et al.* Phys. Rev. **C76**, 064903 (2007).
- [48] I. Kraus *et al.* Phys. Rev. **C79**, 014901 (2009).
- [49] F. Becattini and J. Manninen, J. Phys. **G 35**, 104013 (2008).
- [50] F. Becattini, *et al.*, Phys. Rev. **C 90** 054907 (2014).